EXPERIMENTAL STUDY OF STREAMING FLOWS ASSOCIATEI) WITH ULTRASONIC LEVITATORS

E.H. Trinh and J, I.. Robey a
Jet Propulsion Laboratory
California Institute of Technology

ABSTRACT

Steady-state acoustic streaming flow patterns have been observed during the operation of a variety of resonant single-axis ultrasonic levitators in a gaseous environment and in the 18 to 37 kHz frequency range. light sheet illumination and scattering from smoke particles have revealed primary streaming flows which display different characteristics at low and high sound pressure levels. Secondary macroscopic streaming cells around levitated samples are superimposed on the primary streaming flow pattern generated by the standing wave. These recorded flows are quite reproducible, and are qualitatively the same for a variety of levitator physical geometries. An onset of flow instability can also be recorded in non-isothermal systems such as levitated spot-heated samples when the resonance conditions are not exactly satisfied. A preliminary qualitative interpretation of these experimental results is presented in terms of the superposition of three discrete set of circulation cells operating on different spatial scales. These relevant length scales are the acoustic wavelength, the levitated sample size, and finally the acoustic boundary layer thickness. “l’his approach fails, however, to explain the streaming flow field morphology around liquid drops levitated on Earth. Observation of the interaction between the flows cells and the levitated samples also suggests the existence of a steady-state torque induced by the streaming flows.

a Current address:
Code UG, NASA Headquarters, Washington DC.

1. INTRODUCTION

Acoustic streaming in high intensity standing waves has been extensively investigated, both theoretically and experimentally, Although it is fair to say that a good understanding of the basic nonlinear mechanism at the origin of the generation of the steady-state flows has been obtained [1-5], the *specific* configuration of the flow fields around an ultrasonically levitated sample in a gas has not yet been examined experimentally. In addition, the impact of the streaming flows on the sample mechanical stability as well as on heat and mass transfer processes is just beginning to be documented and assessed[6,7]. In this paper we present what we believe are the first results of experimental studies dealing with the visualization of the macroscopic streaming flow fields induced in an axisymmetric standing wave inside a closed volume. The closed volume is used strictly for the purpose of duplicating real experimental systems and for flow visualization, and it is not a resonant cavity. The standing wave of interest is generated by an ultrasonic driver and a coaxial reflector positioned to induce resonance along the common axial direction, A monotonic radial dependence of the sound field is introduced by both the. curvature of the reflector and by the natural divergence of the radiated ultrasonic beam. "i'he more interesting streaming flows are those around a levitated sample in both isothermal and non-isothermal conditions, although certain characteristics of streaming in an empty chamber have been found to be puzzling and remain unexplained.

The purpose of this communication is to document experimental observations of those specific streaming flows that control the heat transfer mechanism and that could affect the dynamics of solid and liquid samples suspended by a single axis ultrasonic levitator. This is a preliminary investigation which is designed to provide a mostly qualitative assessment of the streaming fields configuration in order to elicit further interest in more detailed and quantitative specific measurements. The emphasis will be placed on *actual experimental systems* for studies in fluid dynamics and materials science using samples levitated in a *gaseous* host medium. The importance of considering actual experimental systems arises from the interaction between the streaming flows induced by the container walls and those caused by the levitated sample itself, This interaction leads to drastically different field configurations depending upon the relative magnitude of these two different streaming fields.

Acoustic levitation has been put to practical use in recent years to study the behavior of free three dimensional liquid surfaces in the form of drops and liquid shells on Earth 8-]0 as

well as in the reduced gravity environment of low Earth orbit where a series of successful experiments has been recently carried out by investigators from Vanderbilt and Yale universities. The results have recently been submitted for publication, and they will presently appear in the open literature. The experimental results to be described below are relevant to space experiments when the sound pressure level is kept in the lower range.

The use of levitated samples to access the metastable undercooked liquid phase has also been successfully demonstrated together with the implementation of remote non-contact physical properties measurement methods [11,12]. The assessment of the influence of the environment on the dynamics and the transport and phase change processes regarding the levitated sample requires the understanding of the characteristics of the induced overall streaming flow fields.

A brief description of the experimental apparatus and of the method is first presented. The results of flow visualization at 37 and 20 kHz are first described for an empty chamber, then with a single levitated, and finally with two levitated samples. Qualitative studies of streaming flows around a heated cylinder are also reported. Preliminary results of Laser Doppler velocimetry measurement of the one-dimensional streaming velocity in an empty chamber at 37 kHz are also presented together with some empirical observation o'f torque generation on a levitated sample through symmetry breaking. Finally, a qualitative interpretation of the experimental evidence is presented based on available theories involving boundary layer streaming around a sphere.

I. THE EXPERIMENTAL APPROACH

A. The apparatus

The more common applications of acoustic levitation have arisen in ground-based laboratories where millimeter-size samples have been suspended with sound at ultrasonic frequencies in either liquid or gaseous host fluids. In a gaseous host medium, typical sound pressure levels (SPLs) are in the 150 to 170 dB range (re. 0.0002 μBar), and the frequency range is roughly between 15 and 50 kHz. In this particular paper, we shall restrict ourselves to experiments at roughly 20, 25, and 37 kHz in a gas host. The basic acoustic configuration of interest is that of the well-known [13-18], nearly one-dimensional "single axis" system where the primary levitation is provided by the radiation pressure arising from

a vertically oriented standing wave, and the centering action arises due to the natural sound beam divergence of the ultrasonic driver as well as due to the curvature of the opposed reflector.

For levitated samples having radii on the order of 1 mm, the product of the wave number and the radius ka = $2\pi a/\lambda = \omega a/c$ is equal to 0.7 at 37 kHz and to 0.37 at 20 kHz. λ is the acoustic wavelength, ω is the acoustic angular frequency, and c is the sound speed in the host fluid. Acoustic pressure will be expressed in this paper in terms of sound pressure level in units of decibels (dB), a logarithmic relative measure with a defined reference pressure p_{ref} = 0.0002 μBar. The sound pressure level is thus: $SPL = 20 \log_{10} p/p_{ref}$, where p is the measured rms acoustic pressure.

Figure 1 is a schematic description of the type of apparatus we have been using in our flow visualization studies. The principal components of the apparatus are the ultrasonic pre-stressed transducer-reflector combination and the sheet illumination. Three different radiating tip shapes have been used, and they range from a circular 12.7 cm aluminum plate at 20.2 kHz, a 4.45 cm diameter steel plate at 25 kHz, to a 1.9 cm diameter straight cylindrical shape at 37 kHz. The vertical ultrasonic standing wave is generated between the transducer radiating face and the opposed reflector which presents a concave axially symmetric curved surface to the incoming wave (the radius of curvature is selected between 3.81 and 7.62 cm depending on the acoustic frequency). The curvature of the reflector produces a radially varying sound pressure distribution which in turn generates a radial restoring radiation pressure force to center the levitated sample close to the central axis. The levitation volume is enclosed by a transparent square or circular cross section chamber. The tracer particles have been generated by burning cotton ropes or incense sticks, and range in size between 0.1 and 10 μm. The scattered light from a 5 mW unpolarized He-Ne beam expanded into a sheet by a long focal length cylindrical lens is observed at an angle between 90 and 1200 from the incoming beam direction in the forward scattering region through a microscope lens at t ached to a video camera.

Figure 2 is a representative plot of the axial and radial acoustic pressure variations as measured by a. probe microphone. in the axial case (Figure 2a), the acoustic pressure was measured along the vertical axis of symmetry and passing through two pressure nodes in the standing wave. For levitation of a solid or liquid sample in a gas environment and in the Earth gravitational field, the equilibrium levitation position is at the pressure nodal planes or below. This distance below the pressure nodal plane is determined by the sound pressure

and the sample density. Very low density materials such as Styrofoam samples and liquid shells are levitated very close to the pressure nodal plane. In the. radial plot (figure 2b), the lateral sound pressure distribution was measured very close to an axial pressure nodal plane. One should keep in mind that the pressure nodal plane corresponds to the acoustic velocity antinodal plane *where the* acoustic velocity amplitude is maximized. Note also that the radial pressure variation with a minimum at the central axis is much men-e moderate than the pressure variation along the vertical direction. This is reflected in a weaker, but still effective radial centering force.

B. The experimental procedure

All measurements were carried out at the ambient temperature of 23 C.

The vertical resonance of the levitation cell is located through a microphone placed flush with the reflecting surface at the axis of symmetry when no sample is levitated. Tuning to resonance conditions simply requires maximization of the microphone signal. When a sample is already levitated in the field, an alternate approach to tune the frequency of the standing wave is to optimize the levitation condition for a given transducer voltage input by maximizing the elevation of the levitated sample. The two methods yield slightl y different resonance frequencies for the standing wave due to acoustic scattering from the sample [19].

The streaming flow field caused by the driver, reflector, and the walls of the enclosure (we call it the primary streaming field) is first studied in order to establish the background flow. The sample is subsequent y introduced and levitated. The new flow field configuration is a resultant of the combination of the primary streaming flow and of the circulation induced by the presence of the sample in the standing wave (we call this circulation the secondary streaming flow field). The changes in the visualized flow fields are then observed as other parameters such as the sound amplitude, the reflector-driver relative alignment, the frequency of the drive, and the size of the sample are varied. “l’he primary streaming flow field arising from the enclosure is generally not considered in theoretical analyses, although its presence is unavoidable in experimental studies. In the case of a heated sample, natural convection must also be taken into account, and the upwardly directed flow of hotter gas will be superposed upon the acoustic streaming flow field.

A simple Laser Doppler Velocimeter (LDV) apparat us designed to measure a single component of velocity, has been used to obtain preliminary values for the streaming velocity in an empty chamber with a standing wave at 37 kHz and at relativel y moderate sound pressure (145 dB). The beam from a 15 mW He-Ne laser was split and then recombined at a determined position in the streaming flow field where the velocity vector was ascertained to be one dimensional and directed vertically. The Doppler frequency was measured by a spectrum analyzer, and the orientation of the measuring laser beams was adjusted to maximize the detected scattered light signal. The same type of smoke used for flow visualization was applied to these LDV measurements. The whole levitator was also translated laterally with respect to the laser beam in order to probe the radial dependence of the streaming velocity. The region of the flow field probed is typically represented by the right lobe of the streaming pattern shown in figure 4a. The LDV was calibrated using a well controlled one dimensional liquid flow where the fluid velocity was measured through independent means.

11. EXPERIMENTAL RESULTS

A. Empty chamber

The flow patterns induced by the reflector, driver, and walls of the enclosure were first investigated in the absence of a sample. At first sight, this would appear to be equivalent to the streaming patterns induced in a resonant chamber (as depicted by Andrade in reference 3), except for a more complicated geometry due to the ultrasonic driver-reflector combination responsible for setting up the standing wave. The results, however, are quite different.

Streaming at 37 kHz was investigated in a levitator shown on the photograph in figure 3. The cylindrically shaped radiating tip (1 .9cm in diameter) is shown facing a 3.175 cm O.D. reflector with a concave face directed towards the levitated liquid sample (radius of curvature is 3.55 cm). The driver-reflector separatism is 1.34 cm, or 1.5 λ (where λ is the acoustic wavelength in air at 37 kHz). The levitated drop of 2mm in diameter is deformed into an oblate spherical shape due to the high acoustic stresses required for levitation in 1G (G being the Earth gravitational acceleration). Surrounding this levitation region, and not shown in the picture, is a square cross-section Lucite enclosure (6,35 x 6,35 x 3.81 cm)

used to slow the smoke dissipation. This enclosure does not significantly influence the primary acoustic field between the driver and reflector at the temperature these experiments were conducted.

Figure 4 shows a photograph of the streamlines of the resulting convective flow at 37 kHz in the absence of a levitated sample and at 145 (figure 4a), 155 (4 b), 158 (4c), 165 dB (4d). The arrows in figure 4b indicate only the direction of the flow, the arrow length does not carry any velocity information, The direction of the flow is *downward* from the reflector to the driver along the central axis, with a returning upward flow on the outer edge of the cells. The direction of this flow is important because it will be superposed upon the streaming convective cells induced when a sample is levitated. The flow is quasi-axisymmetric about the driver-reflector central axis, and the shape of the flow field is therefore roughl y toroidal. At the higher sound pressures shown in figure 4d, the streaming velocity increases, the streamlines become distorted, and the symmetrical character of the flow field degrades. At the highest SPL additional eddies also appear at the velocity antinodal positions along the axis of symmetry. Although these eddies are unstable and periodical] y shed and reform, making them difficult to visualize, their presence is unmistakable with careful observation and tuning of the standing wave. This qualitative change in the morphology of the flow is gradual, building up near the ultrasonic driver where the first set of counter-rotat ing eddies appear.

At 158 dB the acoustic particle velocity (U_{ac}) is 3.9 m/sec and the amplitude (A) is about 100 pm. At 37 kHz the Stokes viscous layer thickness ($\delta = (2\upsilon/\omega)^{0.5}$) is about 11 μm thick (υ is the kinematic viscosity of air and ω is the acoustic angular frequency). For a sample radius a= 1 mm, the ratio of the acoustic particle displacement over the sample radius $\varepsilon = A/a = 0.1$, the ratio of the sample radius over the boundary layer thickness $M = a/\delta =$ 91, and the length scale ratio $\varepsilon.M = A/\delta = 9.1$. Following Gopinath and Mills[6], one can define a "Streaming Reynolds number" as $R_S = \varepsilon U_{ac}\, a/V = \varepsilon^2 M^2 = A^2/\delta^2$. In this particular case, at 145 dB and 37 kllz,Rs='4,7, at 155 dB R_S = 46, at 158 dB Rs = 83, and at 165 dB R_S = 460.

Figure 5 is a reproduction of photographs of streaming flow fields at the two different sound pressure levels of 147 and 154 dB (figure 5a and 5b) and for a 25 kHz levitator characterized by a wider radiating surface (4.45 cm diameter). The enclosure is also larger and cylindrical in shape (7.62 cm diameter and 5.1 cm high). The driver-reflector separation of shout 1.5 wavelengths or 1,99 cm also allows for the levitation of three

separate samples. In this case the flow direction is *vertically* upward along the central axis, and downward along the outer edge of the convection cell, i.e. directly opposite to the particular case of the 37 kHz levitator described previously. The direction of the flow is as indicated by the arrows in figure 5a, and it also applies to figure 5b. An *additional* vortex pair appears, however, by slightly detuning from resonance condition (changing the drive frequency of the ultrasonic transducer). This is shown in figure Sc where the velocity is now downwarid along the central symmetry axis.

This situation is reminiscent of a free acoustic beam traveling down a channel with closed or partially closed end. This case was treated by Nyborg[1] for slip as well as no-slip boundary conditions. According to those predictions, the direction of the flow along the central axis of the channel is away from the sound source for slip boundary conditions and towards the sound source for no-slip conditions. For our experimental conditions, however, the boundary conditions have not changed in such a qualitative manner, Rather, the radius of curvature of the reflector has been found to be the determining factor for the direction of flow: at 37 kHz a reflector with a radius of curvature of 3.55 cm causes the streaming flow to be directed towards the driver (downward) along the central axis, while a reflector with the same outer diameter but with a radius of curvat ure of 7.62 cm will cause a streaming flow in the reverse direction. The circulation direction is also very sensitive to small changes in the acoustic parameters. This is demonstrated by the insertion of an additional vortex pair upon slight modification of the tuning conditions (figure SC).

At relatively low sound pressure (SPL less than 155 dB, $R_S < 46$) onl y a single cell is detected in the vertical direction between the driver and the reflector, although three acoustic half-wavelengths span the same separation. The number of cells in the lateral direction depends on the acoustic pressure level which controls the magnitude of the streaming velocity. The higher the streaming velocity, the wider the two central convection cells become, crowding out the neighboring cells between the enclosure walls and the inner cells. At the SPL of about 154 dB, the central cells will spread out to cover the entire cross section of the enclosed volume. Thus, the point at which the flows reverse depends on the sound pressure level. At the higher sound pressures (SP1.>155 dB), however, the counter-rotating eddies appear at each of the velocity antinodal position within the primary cell. The flow field also takes on a more turbulent character with periodic large scale oscillations having a frequency dependent on the acoustic tuning conditions.

The streakiness shown in the flow visualization photographs is due to inter-particle attraction. This was also observed by Andrade, and it fortuitously helps to visualize. the flow patterns at relatively low sound pressure levels. At higher SPL, however, the flow is of higher velocity and becomes turbulent. The distribution of the particles becomes more uniform as the hydrodynamic force dominates the inter-particle attraction.

The radial distribution of the "streaming velocity" was measured for the flow field shown in figure 4a (SPL=145 dB, R_S = 5) using a basic single velocity component LDV. Figure 6 shows the results of the measurement with the observed streaming velocity plotted as a function of position at a plane midway bet ween the driver and reflector corresponding to the nodes of the cells. A maximum velocity of 3.2 cm/s is found along the central axis, and a third order polynomial tit (continuous line) predicts a reversal of the flow at about 7 mm from the center, in agreement with the flow visualization evidence. The experimental uncertainty under these conditions is estimated to be less than 0.5 cm/s.

B. Streaming around levitated samples in isothermal conditions

Figures 7,8 and 9 reproduce photographs of video images of the streaming flow fields around various levitated samples at 37 kHz. The laser sheet is positioned in order to intersect the sample at its largest cross section, i.e. it slices the sample right at the middle section. A 2 mm diameter Styrofoam ball is shown suspended in the primary streaming field in figure '7. A pair of vortices attached to the upper part of the sample can be faintly seen in this low magnification picture. Figures 8a, 8b, and 8c are higher magnification photographs of levitated liquid shells at three different and increasing sound pressure levels, In addition to flattening the sample, higher sound pressure also increases the size of the secondary vortices. Figures 8d and 8e are even higher magnification views of the liquid shell and of the attached secondary vortices. No *visualization of a smaller scale acoustic boundary layer flow has been obtained.* The flow direction of the secondary vortices is away from the sample along the central axis and toward the sample on the side of the lobes. The primary streaming field direction is still downward along the central axis and upward on the outside lobes. Note that the position of the vortices on the upstream side of the sample is opposite to that found in the classical case of flows past a sphere at intermediate Reynolds number.

The situation is different, however, in the case of a drop which requires sound pressure level of about 165 dB for levitation (R_S = 460). As shown in figure 9a, the secondary

vortices have now been displaced to the lower half of the sample on the downstream side. in figure 9b the laser sheet is offset from the center of the drop and intersects the drop and the attached circulation cells behind the center meridional plane. The three-dimensional circulation cell is donut-shaped, and it is positioned slightly below the drop equator. The primary flow direction is still the same, but the direction in the attached vortices is toward the sample along the center, and away from the sample on the outer lobe. Although the velocity of the primary flow due to the standing wave alone has drastically increased because of the higher sound pressure level required for the levitation of a droplet, the circulation velocity in the lower eddies near the drop is not significantly greater than the upper eddy velocity found in the case of much lighter samples such as Styrofoam balls or liquid shells. Closer inspection of the levitated drop reveals a solid body rotation with its axis directed out of the plane of the photograph, i.e. perpendicular to the acoustic oscillations and to the flows around the sample. The rotation rate is on the order of 1 revolution pcr second.

These secondary vortices are different from the ones described in the preceding section which appear in an empty chamber at the velocity anti nodes at very high SPL. The secondary vortices associated with scattering from the sample are generated even at the lower SPL.

The flow fields characteristic of two simultaneously levitated Styrofoam samples at 20.2 kHz are depicted in figure 10 for three different sound pressure levels. In this case, the radiating surface of the ultrasonic driver is a plate 12,7 cm in diameter driven at resonance with two nodal circles, and the primary streaming ftow direction is the opposite of that obtained at 37 kHz described above. The flow is directed upward along the central axis, and downward on the sides of the convection cell. The secondary vortices are shown attached to the lower half of the samples, and the flow direction is away from the samples along the central axis and toward the samples on the side of the cells. Because of the presence of two samples positioned a half-wavelength apart above and below the pressure antinodal plane, the flow configuration along that plane is visually well defined, A stagnation point is on the symmetry axis and appears to coincide with the acoustic pressure antinode where the flow converges along the central axis (parallel to the direction of the acoustic particle motion) and diverges perpendicular to it.

All samples are levitated near or at the acoustic pressure nodal plane (velocity antinodal plane) in a gaseous environment. Thus all streaming flow configurations visualized with

levitated samples are at or near these planes. Visualization of streaming flows at other positions, was also carried out by using a mechanically suspended sample. As expected, the vortices associated with streaming due. to the sample only appeared as the pressure nodal plane was approached, The first order acoustic velocity vanishes as pressure maxima (velocity nodes), streaming flow should therefore not be observed when the sample is moved to these planes.

C. Streaming around locally heated samples

Practical applications of acoustic levitation include the processing of materials which are spot heated through a focused radiant source[20]. The influence of acoustic streaming on both the tuning of the standing wave and on the forced convective heat transfer motivates the search for an understanding of the macroscopic morphology of these flow fields. Previous researchers have investigated the influence of sound on the heat transfer characteristics of heated cylinders, spheres, and other geometries[21-25] as well as the effects of thermo-acoustic streaming on the acoustic radiation pressure[26]. Qualitative results of the flow visualization of streaming flow fields at 25 kHz around a mechanically held cylindrical] y shaped thermistor (1.9 mm diam., 6.3S mm length) are presented here as preliminary information on the dynamic behavior of the overall macroscopic flow field. The axis of the thermistor is horizontal and perpendicular to the transducer-reflector axis (i.e. perpendicular to the sound oscillations). The thermistor is also used as a variable heat source by establishing a controlled voltage across it, The measurements were again carried out at an ambient temperature of about 23 C.

A quantitative measurement of the effect of an acoustic standing wave on the temperature of a heated thermistor gives an appreciation of the magnitude of the enhancement in convective heat transfer from the sample to the environment, Figure 11 is a plot of the thermistor temperature as a function of the input voltage with and without sound, At the highest initial thermistor temperature of S74 C, an ultrasonic standing wave at 145 dB (R_S = 6.25) will drop the temperature to 427 C, a decrease of 147 C. The total power input to the thermistor in the presence of the standing wave is 2.4 W, while the power required to reach the same temperature in the absence of the ultrasound is 1.6 W. An approximate value for the additional power dissipated through the standing wave is thus 0.8 W. Because the thermistor is located at a acoustic velocity antinode and because of possible interference from acoustic radiation pressure which might directly transfer momentum to a heated gas

due to the impedance mismatch, one cannot assign this enhanced power dissipation to streaming flow effects alone.

The flow pattern for thermo-acoustic streaming in the Earth gravity field is further complicated by the additional contribution from free convection. Furthermore, the interaction between the sound field and the thermal environment requires careful tuning of the acoustic standing wave; slight off-resonance condition will cause flow instability and oscillations. The sequence of photographs reproduced in figure 12 illustrates the typical evolution of the flow field for an heated thermistor (to 130 C) without sound in the Earth gravitational field (figure 12a), then with a heated thermistor and an acoustic standing wave at 150 dB and R_s = 20 (figure 12b), and finally with sound at 155 dB and R_s = 61 (figure 12c). The input of heat allows the formation of t wo full sets of vortices both above and below the cylindrical sample. At higher sound pressure, the above/below symmetry appears to be removed, and the lower eddy pair is stretched outward and split into a pair of counter-rotating, vortices on each side of the sample. With increasing sound pressure level, the outside vortex is further stretched away from the sample, and can be shed under off-resonance condition. Figures 13a through 13d illustrates the periodic instability and vortex shedding induced by off-resonance conditions. The outside vortex of the lower sets periodically stretches to the side and detaches at a low frequency on the order of 1 Hz.

"l-his oscillation and periodic vortex shedding occurs upon slight detuning of the ultrasonic standing wave. (by either changing the. drive frequency or by changing the driver reflector separation distance), but a *steady-state regular* pattern of vortices attached to the thermistor can be obtained by accurate retuning, even though the flow in its immediate vicinity appears disordered and highly turbulent.

Flow visualization with smoke quickly becomes ineffective as flow velocity and disorder increase, but the qualitative picture obtained with these experiments clearly indicates a dramatic increase in convective heat transfer due to thermo-acoustic streaming. Another clear conclusion which can be drawn from these preliminary results is that the tuning of the acoustic resonance conditions is precarious, and that it controls the heat transfer enhancement. A slight detuning from resonance will be amplified by the feedback loop involving the thermal field, and the resulting flow field will be qualitatively altered.

111. DISCUSSION

in view of the evidence presented above, it is quite obvious that in the case of a single axis levitator the outer streaming flow fields generated by the primary standing wave and the physical boundaries strongly modify the local streaming flow configuration around a levitated sample. The superposition of these two flow fields (in addition to that induced by natural free convection) will control the transport processes between the sample and its immediate environment as well as the levitation stability. The resulting flow can therefore be described in terms of juxtaposition of a set of circulation cells on the scale of the levitator (in this case on the order of the acoustic wavelength) with a set of vortices on the scale of the levitated sample. The theoretical understanding of this combination of flows would require, at least in the first approximation, the successive solution of the various streaming and free convective flows. This would also have to be done in the presence of a thermal gradient around the sample in the case of thermo-acoustic streaming. The more recent theoretical treatments[4,7] provide valuable insight on the outer streaming flow and heat transfer around a sphere immersed in an acoustic field, but they still do not include the presence of a background streaming flow field. It is possible, however, to derive a partial qualitative interpretation of the experimental evidence presented above in terms of existing theoretical understanding. This is the motivation for this section of the paper.

A. isothermal streaming in an empty chamber

The standing wave existing between the driver and reflector is a necessary condition for the appearance of steady-state streaming, and the number of half-wavelengths in the standing wave also determines the number of counter-rotating eddies appearing at higher SPL near the velocity antinodes. This is in contrast to the classical case of streaming in a resonant channel (or a Kundt's tube) where a periodic pattern of counter-rotating eddies alternates every quarter-wavelength. The present configuration of a free nearly one-dimensional standing wave unconstrained by side walls appears to be a case exhibiting characteristics which are a combination of the standard solutions for a free traveling wave and a resonant channel mentioned above.

According to the experimental results, a reflector with a smaller radius of curvature will cause the streaming flow to be directed towards the driver along the symmetry axis, while a larger radius of curvature will generate the opposite flow direction. In practice, a smaller

radius of curvature is used to sharpen the radial acoustic radiation restoring force in the velocity antinodal planes. This could be viewed a.. an enhancement of the local static pressure gradient at each velocity antinode. Streaming flows in a standing wave are generally directed towards antinodes along the axis of symmetry. If the velocity antinodes arc more sharply defined close to the reflector because of a smaller radius of curvature, it seems plausible that the flow could preferentially be directed towards the axis of symmetry and away from the reflector along this axis. Preference for a downward flow could be thus explained. Although plausible, this explanation remains somewhat unsatisfactory, and a more detailed investigation of streaming flows along curved boundaries normal to a standing wave is probably required before. this phenomenon can be well understood.

B. Streaming around levitated samples under isothermal conditions,

A straightforward superposition of the primary streaming flow upon the local streaming circulation around a sample can qualitatively account fen- the experimental observations at the lower sound pressure levels. According to Lee and Wang[4] , the outer streaming flow around a sphere right at the velocity antinode consists of two symmetric pairs of counter-rotating eddies. These “outer streaming flows” correspond with what we have defined in this paper as the secondary streaming flows, and they have been thus named in order to distinguish them from the boundary layer flows which are presumed to be much closer to the surface of the sample. It is obvious that the superposition of an axisymmetric larger-scale vortical flows of the types shown in figures 4a-4c and 5a and 5b with these outer streaming flows yields resulting flow fields of the type shown in figures 8 and 10 respectively. A downward directed primary streaming flow past a levitated sphere thus accentuates the upper eddies, creating a stagnation point above the sample, and opposing the return flow of the lower eddies. An upward directed primary streaming flow will result in exactly the opposite flow morphology. In both cases, the direction of flow (away from the sample in the direction parallel to the acoustic oscillations) is still consistent with the predictions of Lee and Wang for the outer streaming flows.

Such a straightforward interpretation is no longer available, however, at very high sound pressure levels when a primary flow field as that shown in figure 4d must be superposed on the outer streaming flow configuration around a sphere, The sense of rotation of the eddies shown in figure 9 is towards the sample in the direction parallel to the acoustic

oscillations, and away from the sample in the direction perpendicular to the acoustic oscillations. In this case, the sample (a liquid droplet) is displaced below the velocity antinode because. of gravity, and according to Lee and Wang, the upper eddies should be accentuated. The fact that experimental observations have revealed an exactly opposite configuration suggests that the primary streaming field plays the dominating role in real experimental systems. It is not clear how the presence of the sample near a velocity antinode affects the generation of the counter-rotating eddies found in a standing wave in an empty chamber. Both a more detailed flow field measurement and a theoretical understanding of the flows found at high sound pressure levels are needed in order to explain the flow field morphology as well as the magnitude of the streaming velocity in the attached eddies in the anomalous case shown in figure 9.

The acoustic streaming field around curved surfaces such as cylinders and spheres has been investigated using boundary layer theory 27-31. The general results have been experimentally confirmed [32,33], and the existence of vortices in the acoustic boundary layer is widely accepted. Figure 14a is a schematic description of the two sets of circulation cells around a spherical sample placed in an acoustic standing wave. The extent of the boundary layer vortices is greatly exaggerated (the acoustic boundary layer thickness is on the order of 10pm at 37 kHz). The secondary macroscopic circulation attached to a levitated sample and experimentally observed in this work, is presumed driven by the inner boundary layer vortices, and any transfer of angular momentum from the fluid to the sample is controlled by this boundary layer circulation the same way that heat and mass transfer between sample and fluid are controlled by the mass diffusion and thermal boundary layers. "1'bus, in addition to the two sets of circulation cells on two different scales mentioned above, the complete description of the sample-fluid interaction should also include the interaction with a third set of circulation cells on the scale of the acoustic boundary layer.

Because of the interaction between the primary and secondary streaming flows it should be possible to modify the configuration of the boundary layer flow field by controlling the macroscopic primary streaming flow field. For example, one might attempt to transfer angular momentum to the levitated sample, i.e. to induce a steady-state torque, by introducing asymmetry in the distribution of the acoustic boundary layer vortices. This could be accomplished by translating the sample from the axis of symmetry of the primary streaming flow field to the region of shear flow. Thus, if a steady-state downward shear flow is superposed on the field depicted in figure 14a, the opposing flow on top of the

sample should remove energy from the upper outer streaming flow eddies as well as from the upper boundary layer vortices as shown schematically y in figure 14b. The upper pair of counter-rotating vortices would also lose strength unequal] y because of the gradient in the velocity field distribution, The lower set of outer streaming eddies would be swept away, and the boundary layer vortices would also gain strength unequally. The result would then be weakened upper boundary layer vortices, with the right upper lobe being less affected. Similarly, the lower boundary layer vortices would be strengthened, with the lower right lobe being less affected. The schematic description of figure 14b would suggest the generation of a torque and rotation of the sample in the clockwise direction.

This has been verified at 37 kHz with the levitation of low density Styrofoam spheres, and by the accurate modification of the relative alignment of the driver and reflector, Figure 15 describes the results: a translation of the driver to the left relative to the reflector induces a clockwise sample rotation, and a translation to the right a counterclockwise rotation. In this situation, the limited translation (up to 5 mm) of the driver does not affect the position of the sample, while the streaming flow field shows a concurrent translation. A translation of the driver to the left would therefore position the levitated sample in the velocity gradient zone closer to the nodal point of the right eddy of the primary streaming flow (see figure 6). The existence of a steady-state torque vector perpendicular to the direction of acoustic oscillations has therefore been demonstrated in a single. axis levitator. The careful observation of higher density levitated liquid drops has also revealed rotation with the angular velocity vector directed perpendicular to the acoustic wave propagation.

These observations are therefore consistent with the suggestion that acoustic streaming-induced flows in an axisymmetric system can introduce a steady-state torque on a levitated sample when symmetry in the spatial distribution of the outer streaming flow field around a spherical sample is removed by a background flow field. A corollary question more relevant to practical applications of acoustic positioning, is whether the conditions of symmetry can ever be fulfilled in order to avoid the generation of extraneous torque.

C. Streaming around locally heated samples

Even at lower sound pressure level the thermo-acoustic streaming flow field reveals itself to be quite complex. This is partially due to the additional convective circulation introduced by the gravitational field. A qualitative change in the flow field configuration is dramatically

illustrated by the splitting of the lower set of eddies, the stretching of the outermost eddy, and the vortex shedding upon oscillation of the acoustic field, Such a transition to different flow regimes has been found by other workers [25] at lower frequency (1 kHz): laminar to vortex shedding to turbulent regime transitions as the sound pressure increases have been documented experimentally using holographic interferornetry and heat transfer parameter correlation. 1 n our case, the transition to the vortex shedding regime is obtained only under specific acoustic tuning conditions.

A rough comparison between the heat transfer measurements obtained in this work with the theoretical approach of Gopinath and Mills [6] can only be carried out for the lower temperature results since their results have been derived under this assumption. With a temperature difference of ΔT = 130 C between the thermistor and its environment, the power input was Q = 0.199 W. For a sound pressure level of 145 dB, the streaming Reynolds number R_s is 6.5. Assuming the thermistor is isothermal, the average heat transfer coefficient h can be calculated for a cylinder of radius a and length 1. with $h = Q / 2\pi aL\Delta T$. The Nusselt number Nu can then be calculated using $Nu = 2ha / K$, based on the thermistor radius and where K is the air thermal conductivity. Using the correlation suggested in reference 6, the coefficient $C = Nu / (R_s)^{1/2}$ is calculated to be 1.17. 'I'he relevant theoretical result derived for large streaming Reynolds number is 1.10. Using our results for ΔT= 427 C, however, yields a coefficient C = 4.3. A satisfactory agreement is obtained for relatively *low sound pressure level and small temperature difference* although the experimental streaming Reynolds number is only equal to 6.5.

SUMMARY

We have reported the results of acoustic streaming flow visualization characteristic of ultrasonic levitators operating in the Earth gravitational field. In addition to the relevance of streaming to practical applications of acoustic levitation, the interesting properties of these flows are of fundamental interest in themselves, and we hope to provide the motivation for theoretical undertakings directed towards this subject.

The isothermal streaming flow field in a closed chamber with an ultrasonic sound source facing a reflector initially takes on the appearance of fairly symmetrical and laminar primary convection cells on the spatial scale of the sound wavelength at low sound pressure. It displays, however, fine structures in the form of imbedded eddies separated by a half-

wavelength and centered on velocity antinodes at higher sound pressure. The sense of rotation of these primary cells appears to depend on the geometry of the levitator. As the sound pressure is further increased, the flow field takes on a disordered and seemingly turbulent appearance with oscillations detected for specific acoustic settings.

When samples are levitated, the primary circulation combines with the secondary streaming attached to the samples and having spatial dimension on the scale of the sample size. At lower sound pressure, a simple superposition of the two flows appears to qualitatively explain the morphology of the resulting flow. At higher sound pressure this is not sufficient because the interaction of different eddies is not straightforward to analyze, and more detailed experimental and theoretical studies are required for an understanding of these phenomena, A simple qualitative model of the interaction of the different streaming flows at the lower sound pressures suggests the generation of a steady-state, flow-induced torque on the levitated sample when perfect symmetry is no longer present.

‘l’he streaming flows around a heated sample placed in an isothermal environment have also been visualized and the modification in the heat transfer characteristics by the sound field has been cursorily examined, It appears that the low temperature measurement obtained in this work is in agreement with results of computations by Gopinath and Mills for small temperature difference. Existing evidence of substantial acoustic enhancement of heat transfer processes has been confirmed by the fluid flow and heat transfer process observed here.

ACKNOWLEDGMENT

The research described in this paper was carried out at the Jet Propulsion Laboratory, California Institute of Technology, under contract with the National Aeronautics and Space Administration. We gratefully acknowledge Mr. Marc Gaspar's contribution in the measurement of the streaming velocity using the Laser Doppler Velocimetry apparatus.

REFERENCES

1. W.L.Nyborg, "Acoustic Streaming," in *Physical Acoustics,* edited by W.P. Mason (Academic Press, New York, 1965), vol. IIB, Chapt. 11, pp. 265-331.

2. M.J. Lighthill, J. Sound Vib. 61, 391-418 (1978)

3. E.N. da C. Andrade, "On the circulation caused by the vibration of air in a tube", Proc. Roy. Sot. (London) 134A, 445-470 (1931).

4, C.P. Lee and T.G. Wang, "Outer acoustic streaming", J. Acoust. Sot. Am. 88, 2357-2375 (1 990).

5. C.P. Lee and T.G. Wang, "Near-boundary streaming around a small sphere due to two orthogonal standing waves", J. Acoust. Sot. Am, 85, 1081-1088 (1988).

6. A, Gopinath and A.F. Mills, "Convective heat transfer from a sphere due to acoustic streaming", J. Heat Transfer, 11S, 332-341 (1993).

7. A. Gopinath and S.S. Sadhal, "Thermoacoustic streaming effects from a sphere subject to time-periodic temperature disturbances", preprint submitted to the Int. Heat and Mass Transfer Conference, Brighton, UK (1994).

8.];.11. Trinh, "Fluid Dynamics and Solidification of Levitated Drops and Shells" in *Progress in Astronautics and Aeronautics,* Edited by J.N. Koster and R. I.. Sani, vol. 130, pp. 515-536 (1990).

9. E.H. Trinh, J. Robey, A. Arce, and M. Gaspar, "Experimental studies in fluid mechanics and materials science using acoustic levitation", Mat. Res. Sot. S ymp. Proc., Edited by P. Nordine, vol. 87, pp. 5"1-69, Materials Research Society publication (1 987).

10. A. Biswas, E.W. Leung, and E.H. Trinh, "Rotation of ultrasonically levitated glycerol drops", J. Acoust. Sot. Am., 90, 1502-1S08, (1991).

11.101. Trinh, P.L. Marston, and J.L. Robcy, "Acoustic measurement of the surface tension of levitated drops", J. Colloid Interface Sci., 124, 95-103, (1988).

12. E.H. Trinh, "Levitation studies of the physical properties and nucleation of undercooled liquids", *Proceedings With European Symposium on Materials and Fluid Sciences in Microgravity,* Oxford, UK 1989, European Space Agency publication SP-29S, pp. 503-508 (1989).

13. A.R. Hanson, E.G. Domich, and H.S. Adams, Rev. Sci. Instrum. 35, 1031 (1964).

14. E.G. Lierke, R. Grossbach, K. Flogel, and P. Clancy, in *IEEE Proceedings on Ultrasonics,* Edited by B.R. McAvoy (IEEE, New York 1983), Vol. *2,* pp. 1130-1139.

15. R.R. Whymark, " Acoustic field positioning for containerless processing", Ultrasonics 13, 251 (1975).

16. E.H. Trinh, " Compact acoustic levitation device for studies in fluid dynamics and material science in the laboratory and in microgravity", Rev. Sci. Instrum. S6, 2059-2065 (1985).

17. Y. Tien, R.G. Holt, and R.E. Apfel, "Deformation and location of an acoustically levitated drop", J. Acoust. Sot, Am, 93, 3096 (1 993).

18. C.P. Lee, A.V. Anilkumar, and T.G. Wang, "Static shape and instability of an acoustically levitated drop", Phys. Fluids A *3,2497 (1991).*

19. E. Leung, C.P. Lee, N. Jacobi, and T.G. Wang, "Resonance frequency shift of an acoustic chamber containing a rigid sphere", J. Acoust. Sot. Am. 72,615-620 (1982)

20. J. Magi]], F. Capone, R. Beukers, P. Werner, and R.W. Ohse, "Pulsed laser *heating* of acoustically levitated microsphere under pressure", High Temps.-High pressures, 19, 461-471 (1987)

21. R.M. Fand, "Mechanism of interaction between vibrations and heat transfer", J. Acoust. Sot. Am. 34, 1187-1894 (1962)

22. P.D. Richardson, "Heat transfer from a circular cylinder from acoustic streaming", J. Fluid Mech. 30,337-355 (1967)

23. B.J. Davidson, "Heat transfer from a vibrating circular cylinder", Int. J. Heat Mass Transfer, 16, 1703-1727 (1973)

2.4. W.A. Oran, W.K. Witherow, and B.B. Ross, "Some limitations on processing materials in acoustic levitation devices", *Proceedings 1979 Ultrasonics Symposium,* IEEE Symp. Proceedings, 482-486 (1979)

2S. E.W. Leung, E. Baroth, C.K. Chan, and T.G. Wang, "Thermal acoustical interaction and flow phenomenon", *Third International Conference on Drops and Bubbles,* AIP Conference Proceedings 197,58-70 (1989)

26. C.P. Lee and T.G. Wang, "Acoustic radiation force on a heated sphere including effects of heat transfer and acoustic streaming", J. Acoust. Sot. Am, **83,** 1324-1331 (1988)

27.11. Schlichting, "Berechnung ebener periodischer Grenzschichtstromungen" (Calculation of plane periodic boundary layer streaming), Phys. unserer Z. 33,327-335 (1932)

28. W.P. Raney, J.C. Corelli, and P.J. Westervelt, "Acoustic streaming in the vicinity of a cylinder", J. Acoust. Sot. Am. 26, 1006 (1954)

29, C.A. Lane, "Acoustical streaming in the vicinity of a sphere", J. Acoust. Sot. Am, 27, 1082 (1955)

30. C.Y. Wang, "The flow field induced by an oscillating sphere", J. Sound Vib. 2,257 (1965)

31. N. Riley, "On a sphere oscillating in a viscous fluid", Quart. J. Appl. Math., 19,461 (1966)

32. J. Holzmark, 1. Johnsen, T. Sikkeland, and S. Skavlem, "Boundary layer flow near a cylindrical obstacle in an oscillating incompressible fluid", J. Acoust. Sot. Am. 26,26-39 (1954)

33. J.D. West, “Circulation occuring in acoustic phenomena”, Proc. Phys. Sot. 1164,483 (1951)

FIGURE CAPTIONS

Figure 1.

Schematic representation of the experimental apparatus. An ultrasonic single-axis levitator consisting of a driver and a reflector generates a standing wave between the driver-reflector gap. A streaming flow field induced by the high intensity acoustics can be visualized by illuminating entrained smoke particles. The flow pattern is recorded through a video camera (not shown).

Figure 2.

Plots of the measured sound pressure profiles in the vertical (a) and lateral direction (b). 'l'he voltage output of the microphone is plotted as a function of the distance from the radiating face of the ultrasonic driver (a) or as a function of the lateral distance accross the radiating face (b). The results of the measurement of the lateral profile in figure 1 b has been obtained at a plane near the velocity antinodal (pressure nodal) plane. These particular measurements have been obtained with the use of a 12.7 cm diameter radiating plate, but the pressure distribution is qualitatively similar for radiating plates of other geometries.

Figure 3.

Close-up photograph of a 37 kHz levitator. Shown arc the cylindrically-shaped radiating tip (1.9 cm diam.), a spheroidally-shaped levitated liquid drop (about 0.2 cm diam.), and the reflector (3. 1'75 cm diam.).

Figure 4.

Photographs of smoke streaklines in a 37 kHz levitator at 145 dB (a), 155 dB (b), 158 dB (c), and 165 dB (d). The laser light sheet (0.5 mm thick) is positioned in a meridional plane of the axisymmetric flow pattern. Only shown are the main lobes of the circulation cells. These lobes grow wider with increasing sound pressure. At the highest SPI. the streamlines are distorted and embedded sets of counter-rotating vortices appear near the velocity antinodes (d). The direction of the circulation is counterclockwise for the right main circulation cell with the direction of the flow downward along the central symmetry

axis. The circulation direction of the left main cell is symmetric m the right lobe circulation with respect to the central axis.

Figure S.

Photographs of circulation patterns in a 25 kHz ultrasonic levitator at 147 dB (a) and 154 dB (b). The circulation direction is clockwise for the right main lobe. Upon slight detuning in frequency of the driver, the circulation direction in the center of the levitator is reversed. An additional set of circulation cells is inserted with flow directed downward along the central axis of symmetry.

Figure *6.*

Experimental results of the one dimensional streaming velocity measurement in a 37 kHz levitator. The measurement was carried out with a laboratory-built laser Doppler velocimeter for the right circulation lobe at 145 dB (see figure 4a). The velocity was measured in a fixed horizontal plane as a function of the distance from the central axis of symmetry. The curve drawn through the data points is just a least square fit. The velocity is maximum at the center, and continuously decreases to zero with radial distance from the center until the point of flow reversal is reached.

Figure 7.

Photograph of flow patterns around a 2mm diameter levitated Styrofoam sample at 37 kHz. The primary circulation ceils are still visible, and attached secondary eddies can be faintly seen on the upper half of the levitated sample.

Figure 8.

Photographs of higher magnification views of a levitated of 3 mm diameter liquid shell at 37 kHz. The attached secondary eddies grow in extent, and the sample is flattened as the the sound pressure level is increased (a to c). The secondary circulation cells are counter-rotating, and the streaming velocity is directed away from the liquid shell along the central axis. An even higher magnification view of the attached vortices is shown in figures 8d and 8e.

Figure 9.

Photographs of streaming flow pattern around a 2 mm diameter levitated drop at 37 kHz. The attached eddies have moved to the lower half of the drop even though the direction of the primary cell circulation has not changed, The laser sheet is positioned at the center meridional plane of the drop in a, but it is translated behind this plane in b.

Figure **10.**

Photographs of the flow pattern in a 20.2 kHz levitator without a levitated sample (a), and with two 2 mm diameter Styrofoam balls at increasing sound pressure level (b to d). The primary circulation direction is now clockwise in the right lobe with upwardly directed velocity along the central axis of symmetry. The attached secondary eddies are situated at the lower half of both of the levitated samples. A stagnation point is clearly visible between the two spheres in the vicinity of the pressure antinodal plane.

Figure 11.

Plot of thermistor temperature as a function of input voltage in the absence of ultrasound (*) and with acoustic drive at 14S dB (o). The thermistor is used as a heater, and the effect of streaming can be measured by the temperature decrease for each voltage setting,

Figure 12.

Air flow patterns around a heated cylindrically shaped thermistor (1.9 mm in diameter and 6.35 mm long) in free convection without ultrasound (a), with a standing wave at 150 dB (b), and finally with acoustics on at 155 dB(c). In this particular case the primary streaming flow cells in the absence of the sample are directed downward along the central axis, i.e. an unheated sample would display streaming-induced circulation cells on the lower half of its cross-section,

Figure 13.

Photographs of streaming flow patterns around a heated cylindrically-shaped thermistor at various stages of the vortex shedding instability. The sequence (a)-(c) depicts the stretching of the lower vortex pairs (a and b) and the shedding of the outermost cell. The last

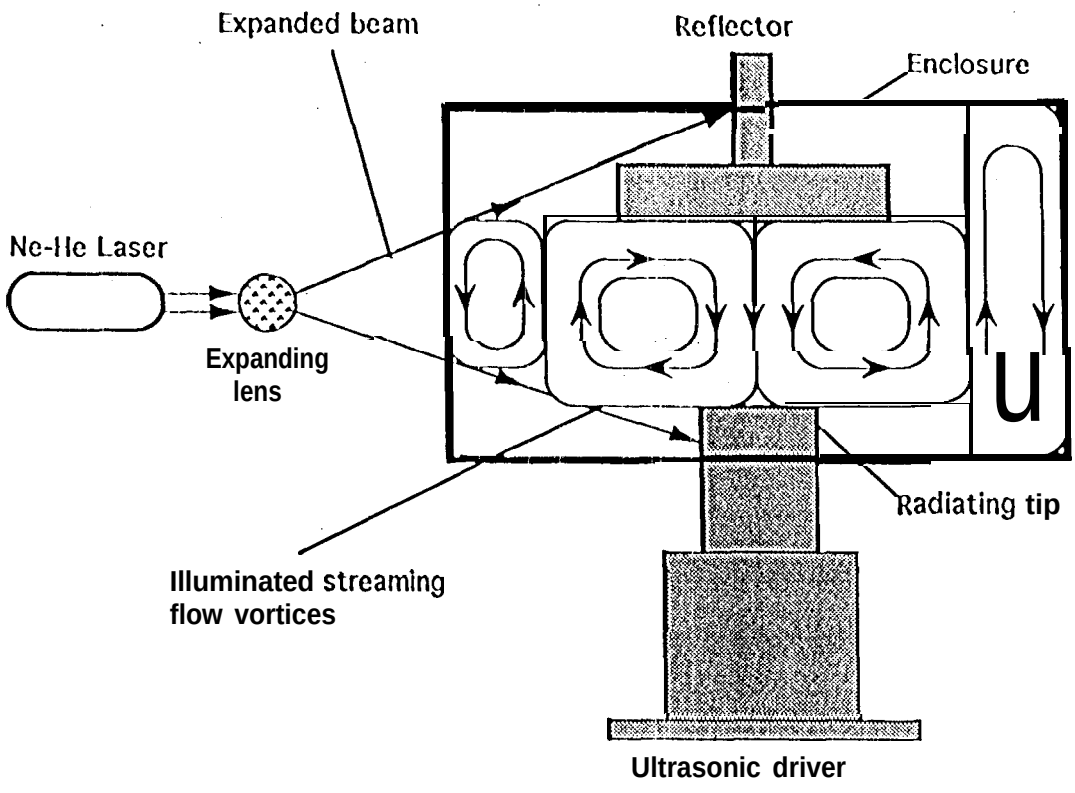

Figure 1.

Schematic representation of the experimental apparatus. An ultrasonic single-axis levitator consisting of a driver and a reflector generates a standing wave between the driver-reflector gap. A streaming flow field induced by the high intensity acoustics can be visualized by illuminating entrained smoke particles. The flow pattern is recorded through a video camera (not shown).

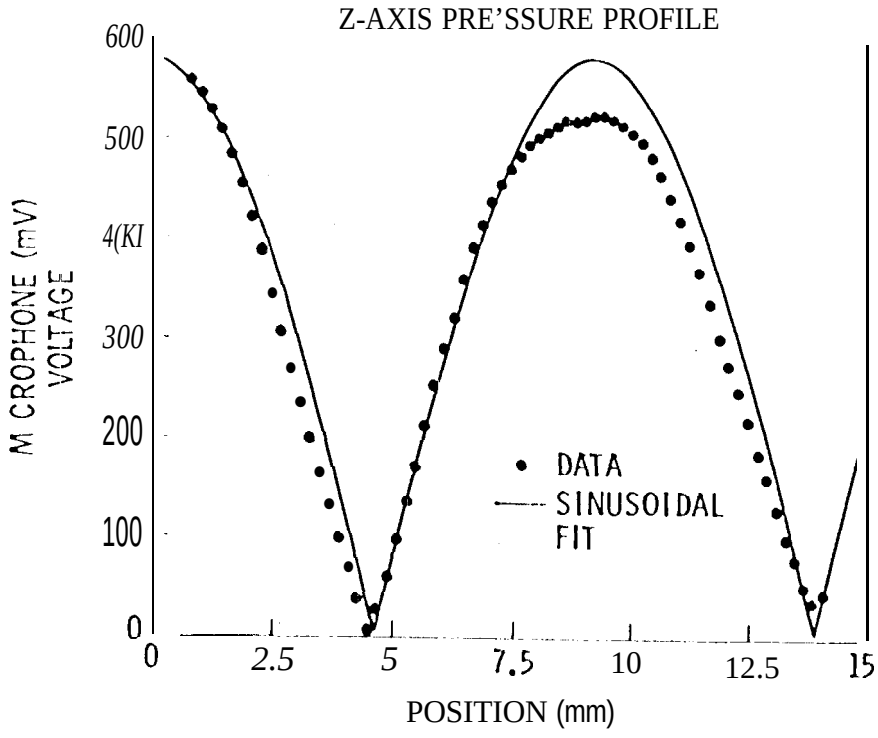

a

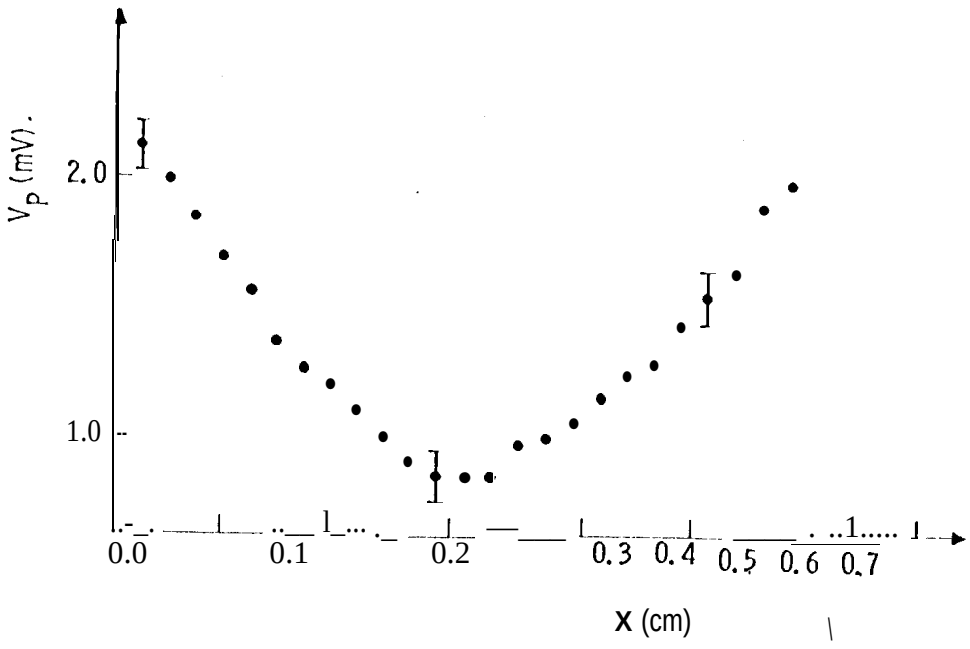

b

Figure 2.

Plots of the measured sound pressure profiles in the vertical (a) and lateral direction (b). The voltage output of the microphone is plotted as a function of the distance from the radiating face of the ultrasonic driver (a) or as a function of the lateral distance accross the radiating face (b). The results of the measurement of the lateral profile in figure 1b has been obtained at a plane near the velocity antinodal (pressure nodal) plane. These particular measurements have been obtained with the use of a 12.7 cm diameter radiating plate, but the pressure distribution is qualitatively similar for radiating plates of other geometries.

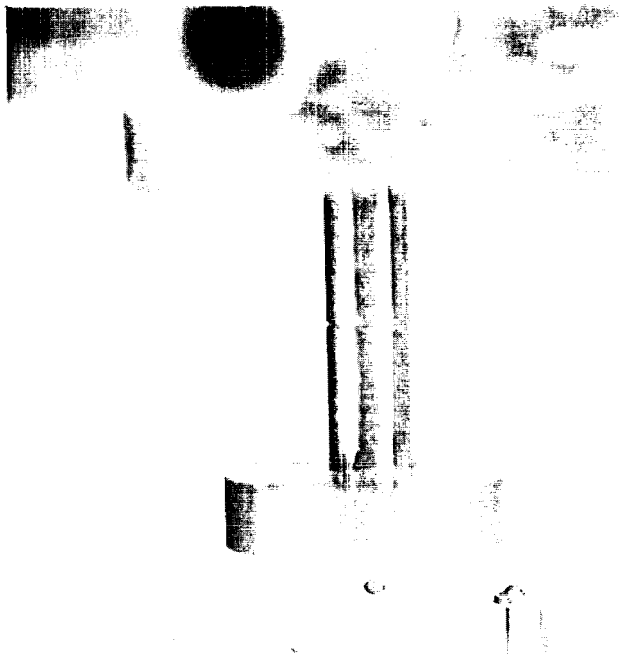

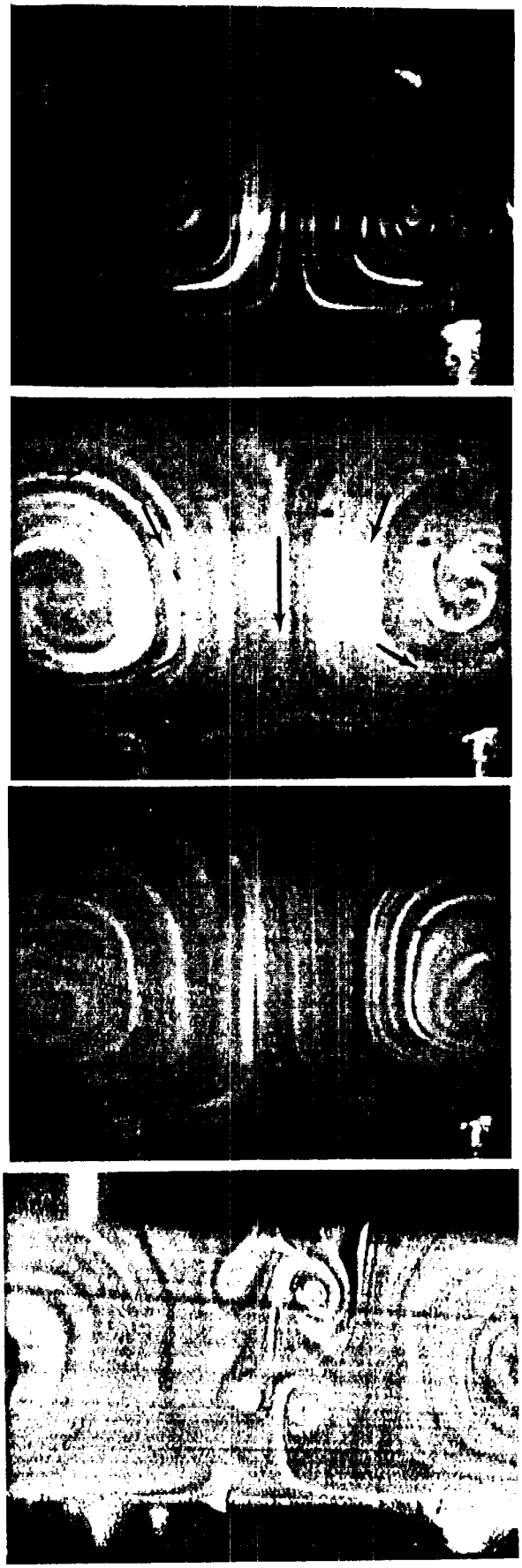

Fig. 1.

a

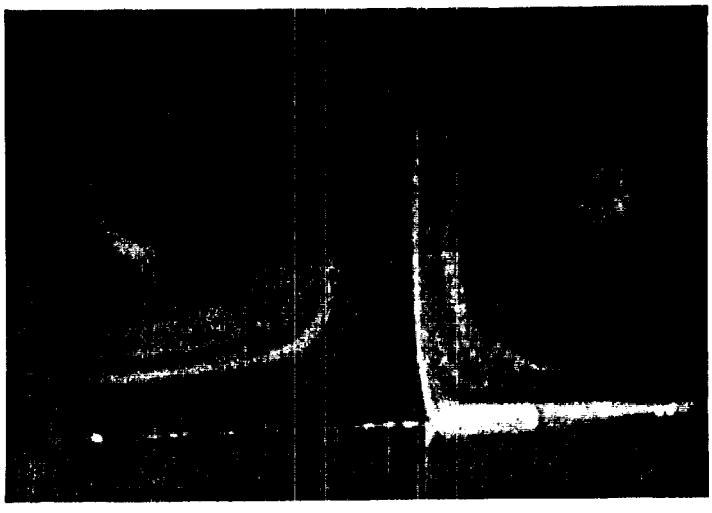

b

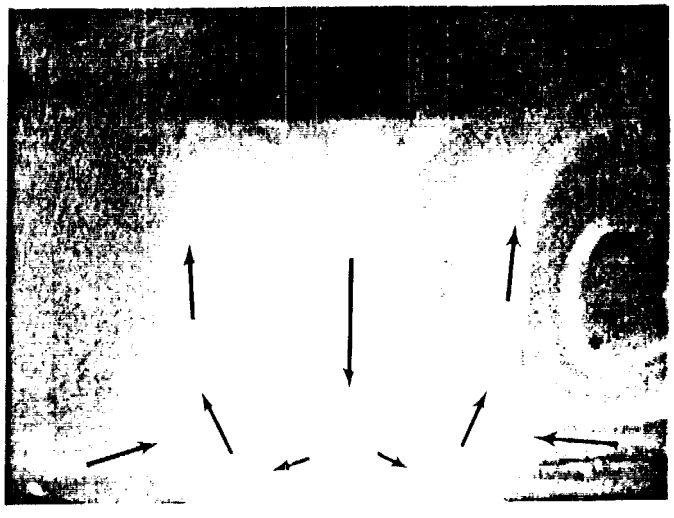

c

Fig. 5

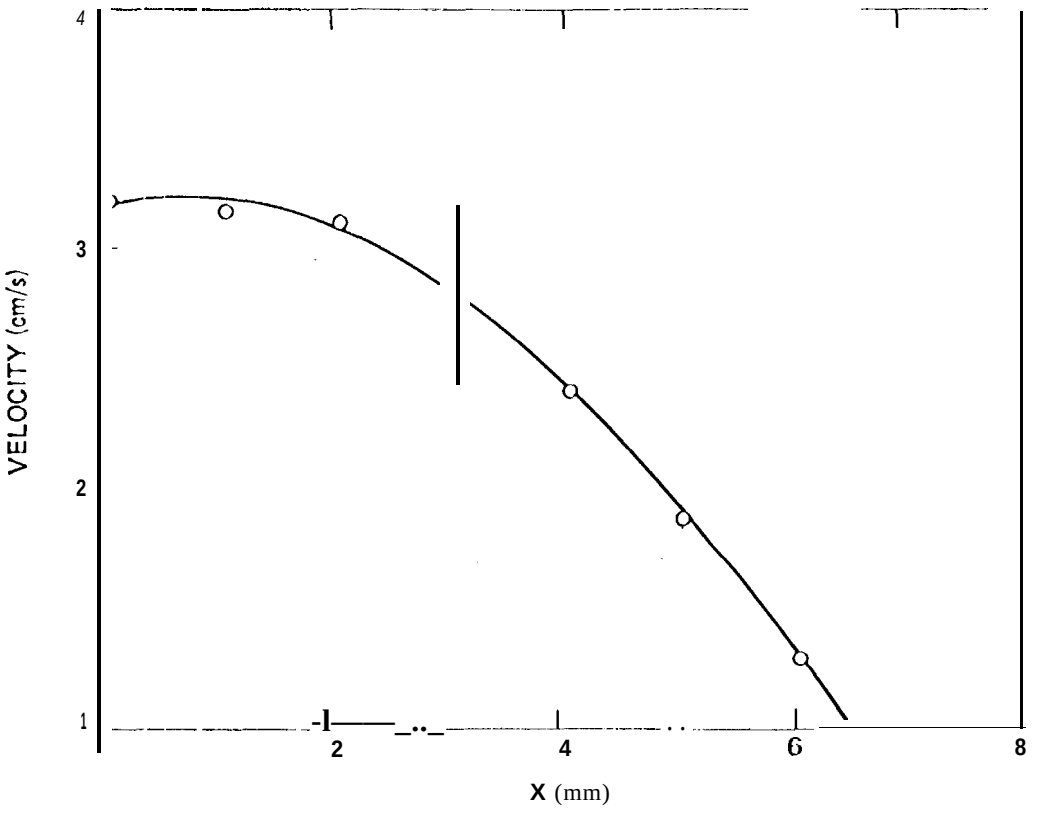

Figure 6.

Experimental results of the one dimensional streaming velocity measurement in a 37 kHz levitator. The measurement was carried out with a laboratory-built laser Doppler velocimeter for the right circulation lobe at 145 dB (see figure 4a). The velocity was measured in a fixed horizontal plane as a function of the distance from the central axis of symmetry. The curve drawn through the data points is just a least square fit. The velocity is maximum at the center, and continuously decreases to zero with radial distance from the center until the point of flow reversal is reached.

a

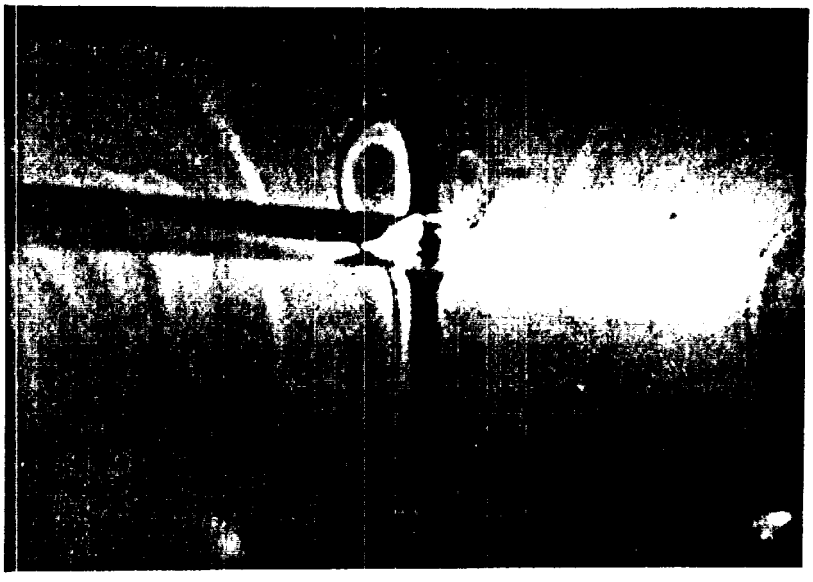

b

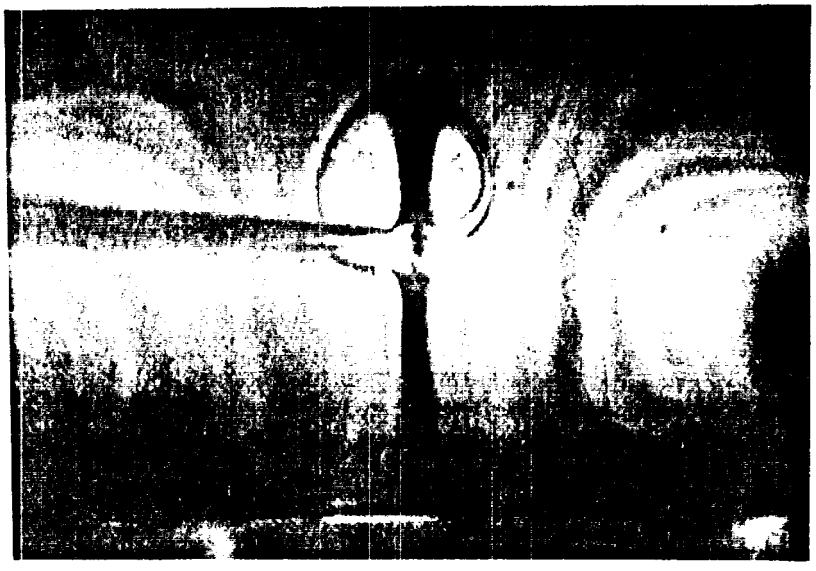

c

Fig. 8

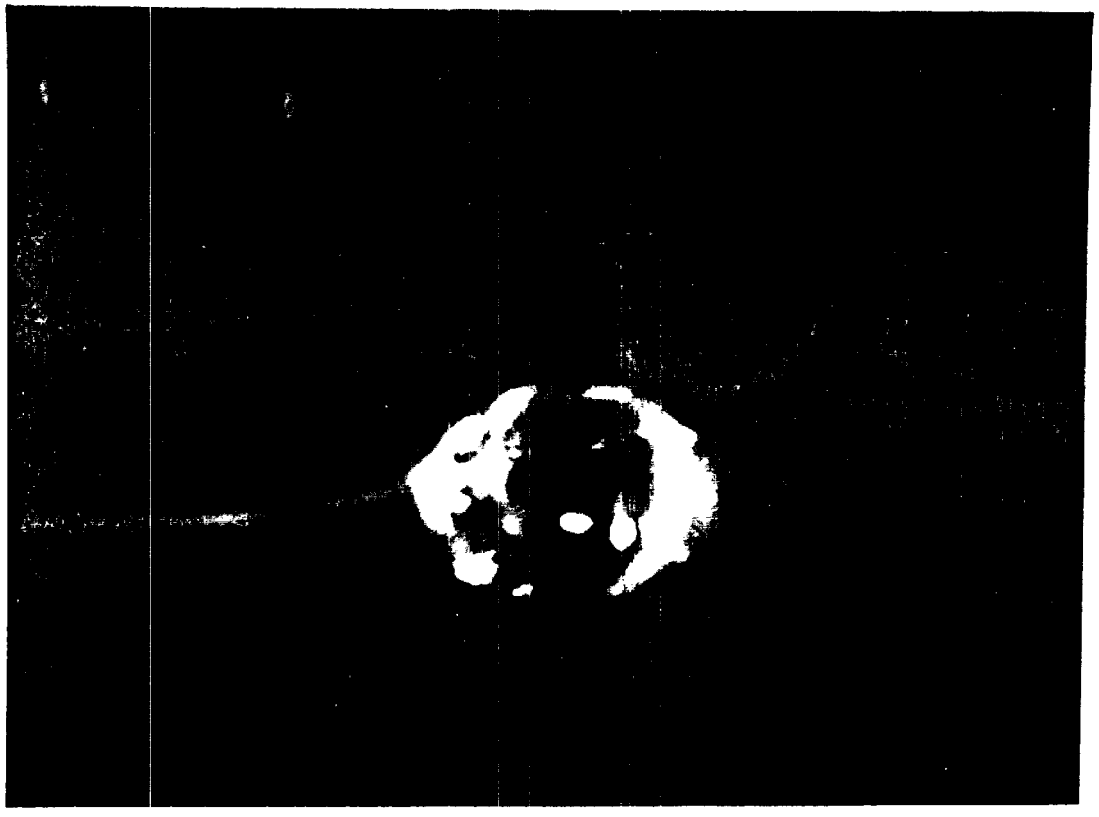

d.

e

Fig. 8

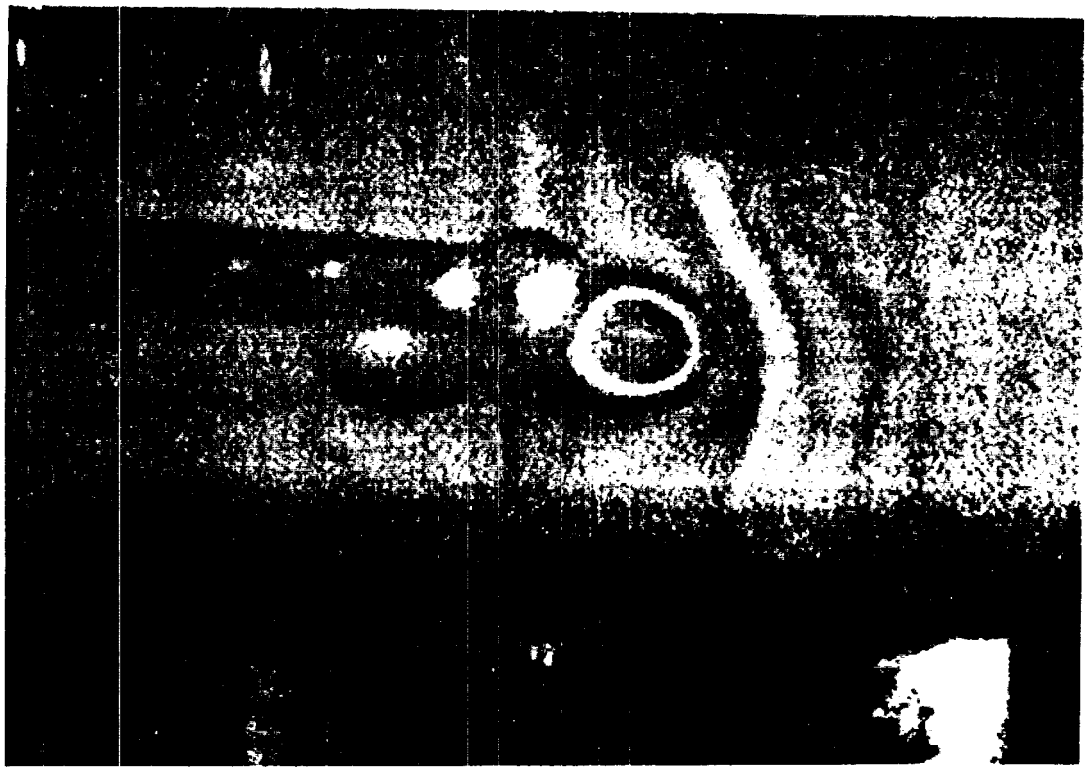

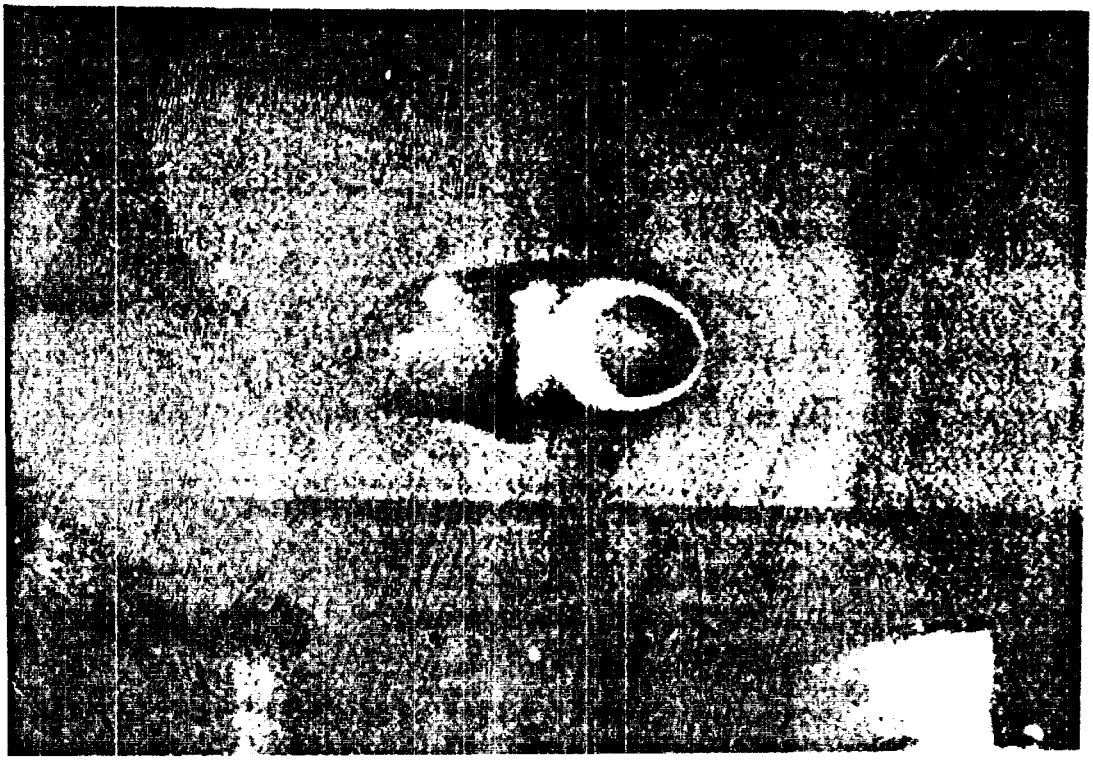

Fig. 9

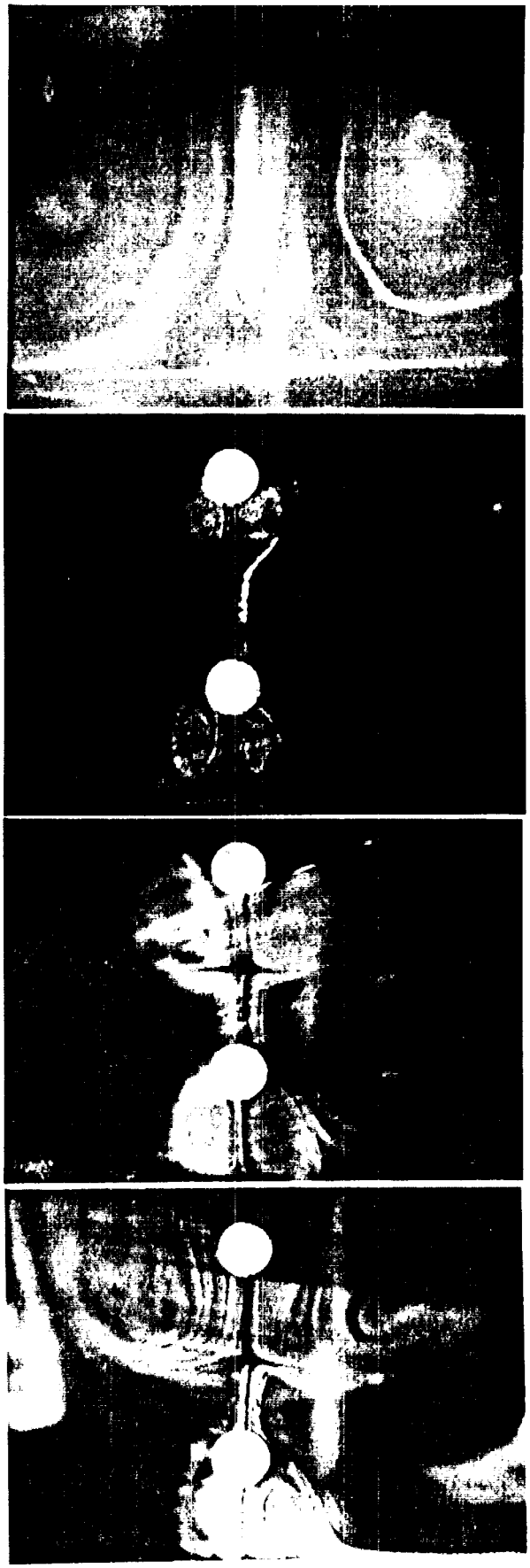

Fig. 10

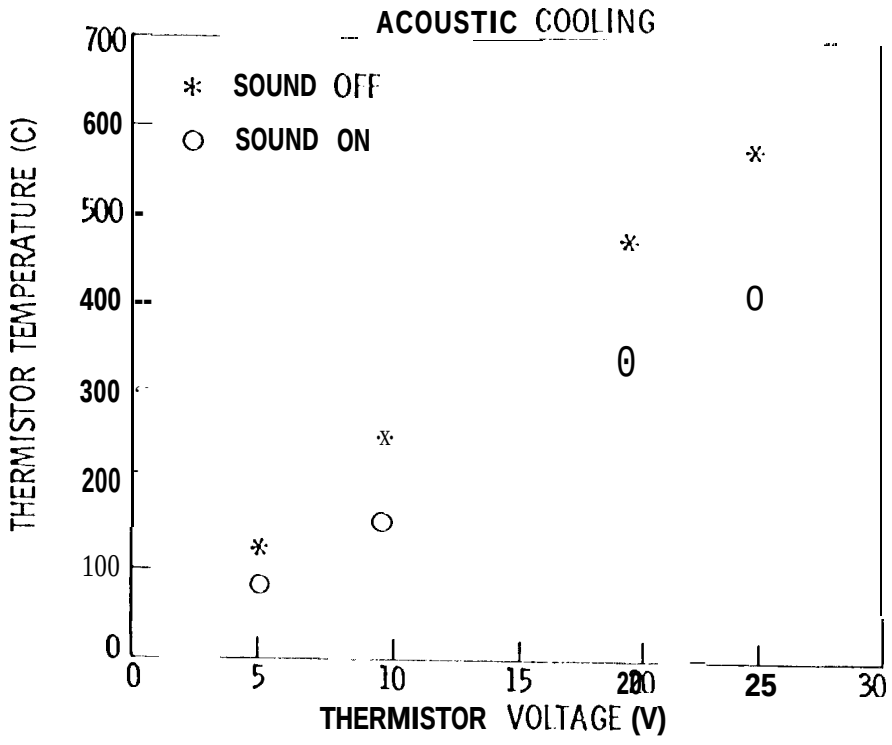

Figure 11.

Plot of thermistor temperature as a function of input voltage in the absence of ultrasound (*) and with acoustic drive at 145 dB (o). The thermistor is used as a heater, and the effect of streaming can be measured by the temperature decrease for each voltage setting.

a

b

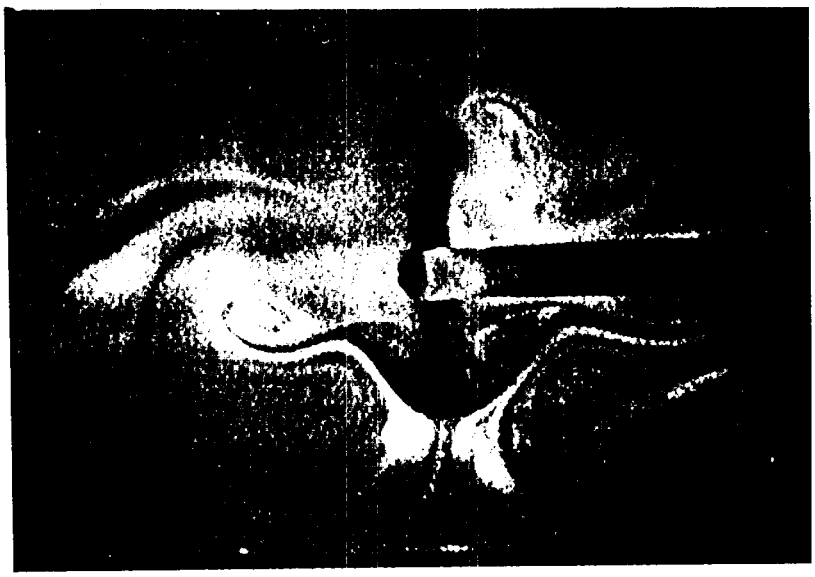

c

Fig. 12

A

B

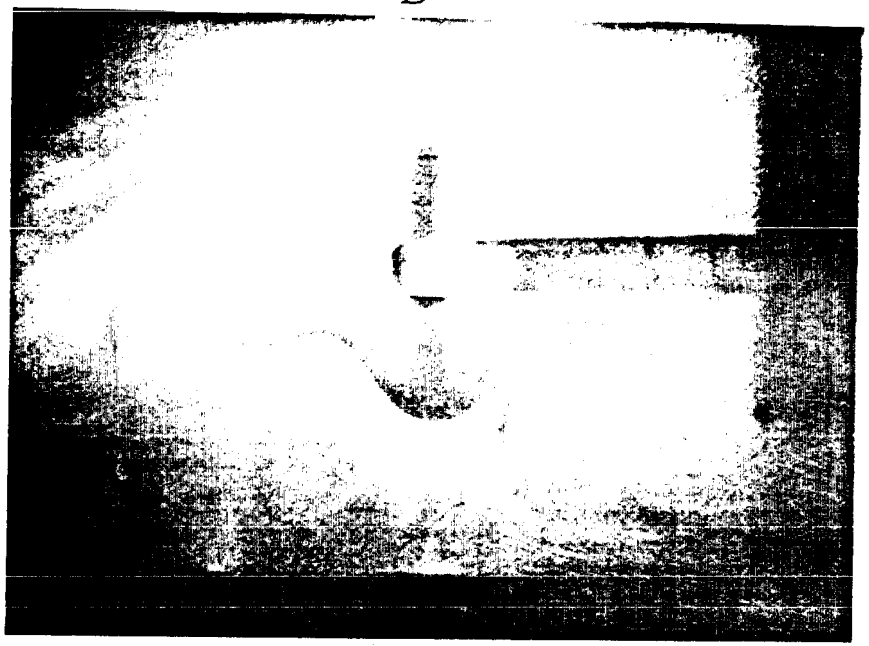

C

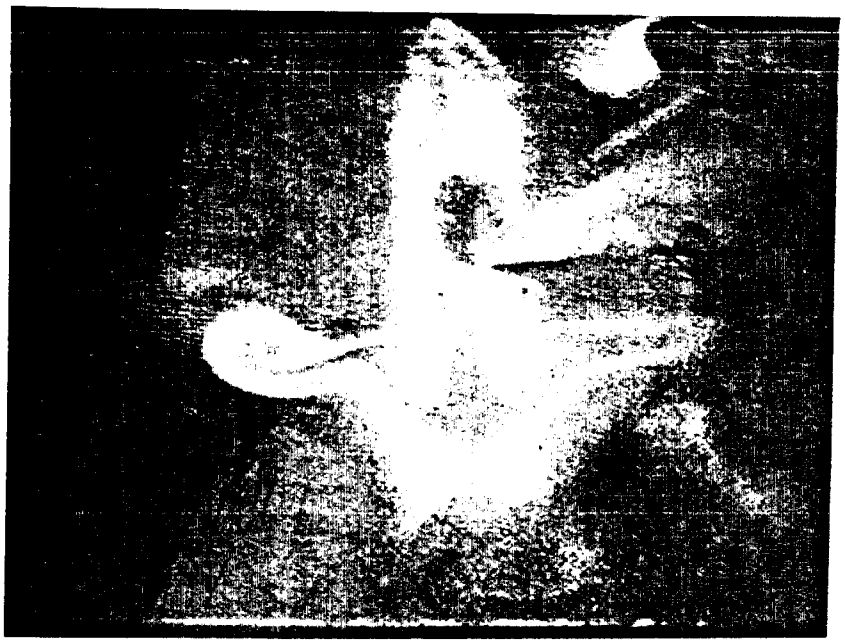

D

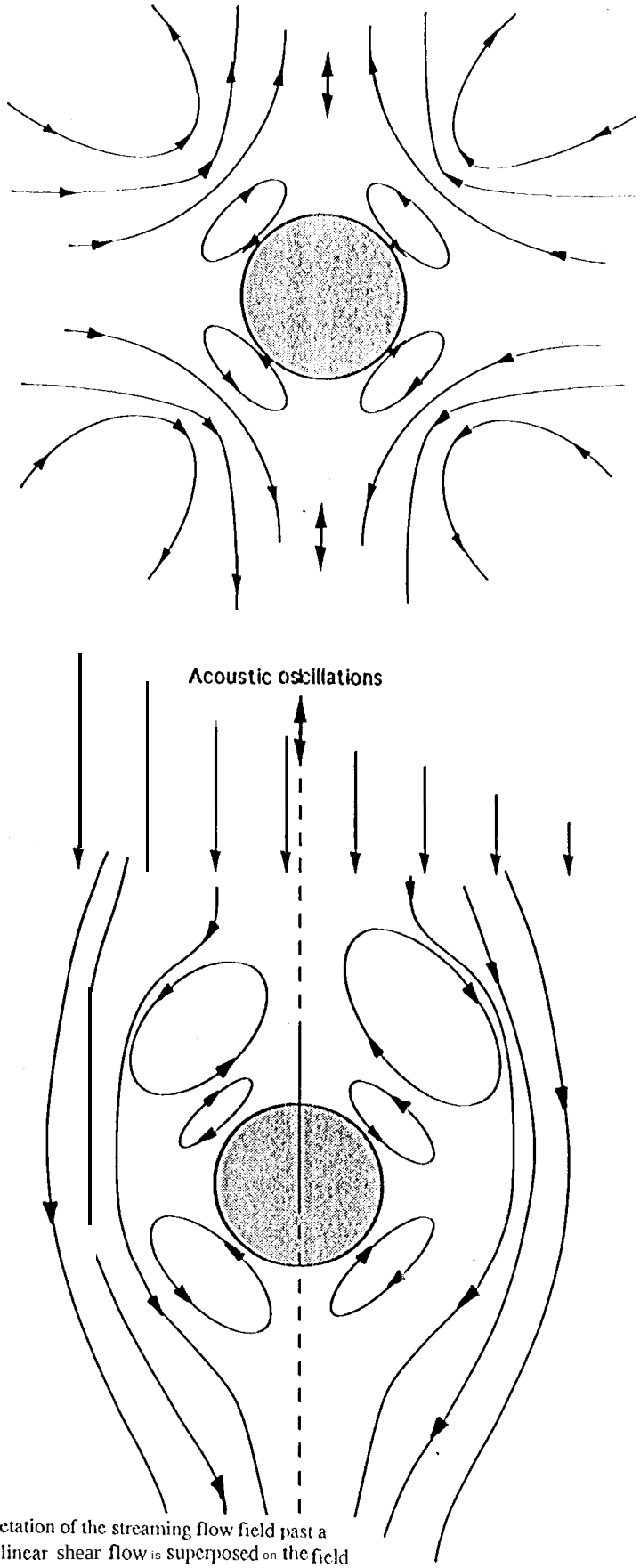

Figure 14.

Schematic description of the theoretical interpretation of the streaming flow field past a sphere using existing models (a). in (b) a rectilinear shear flow is superposed on the field of (a), and an interpretation of the resulting flow field is suggested, Because of the velocity gradient in the additional flow, both the outer vortical as well as the boundary layer flows are affected unequally. This could give rise to the loss of axial symmetry and the generation of a steady-state torque on the sample. In this particular case, a clockwise rotation of the

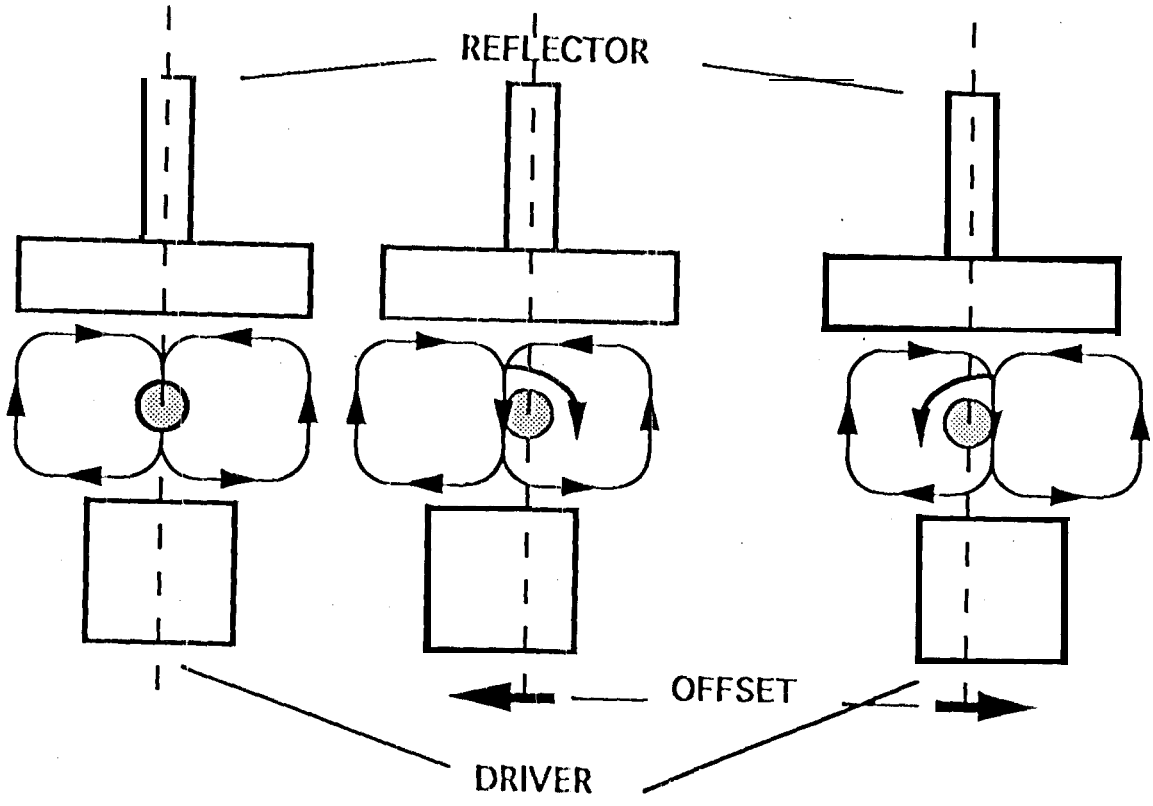

Figure 1 5.

Schematic description of the observed torque generation phenomenon in a single axis ultrasonic levitator. As the. driver and reflector are aligned with respect to each other, the sample and the primary flow cells are symmetrically positioned, and a levitated Styrofoam sample is not rotating. As the driver is displaced to the left with respect to the reflector, the sample remains locked to the reflector, but [he. flow cells shift in unison with the drivel. A resulting clockwise rotation (the angular velocity vector is directed into the page) is observed. The opposite rotation is observed as the. driver is shifted to the right of the reflector.